Study of the thermal degradation of bioactive sol–gel coatings for the optimization of its curing process

M. Hernández -Escolano[1*], X. Ramis[2], A . Jiménez-Morales[3], M. Juan-Díaz[4], J. Suay[1,4]

[1]Centre for Biomaterials and Tissue Engineering, Univ. Politec Valencia, C/Ingeniro Fausto Elio S/N, 46021 Valencia, Spain

e-mail: miheres@doctor.upv.es URL: http://www.upv.es/cb/

[2]Laboratory of Thermodynamics, Univ. Politec. Cataluña, Av. Diagonal 647, 08028 Barcelona, Spain

[3]Universidad Carlos III, Av. Universidad 30, 28911 Leganés, Madrid, Spain2

[4]Universidad Jaume I, Vicent Sos Baynat, s/n, 12071 Castelló de la Plana, Spain

Abstract: A set of materials has been prepared by sol–gel process containing different quantities of hydroxyapatite (0, 2.5 and 5% HAp w/w) using as silica precursors glycidyloxypropyltrimethoxysilane (GPTMS) and tri-ethoxyvinylsilane (VTES). In order to optimize the curing process to obtain sintherized systems (inorganic network) or hybrid systems (organic–inorganic) a TG and FTIR studies have been developed and degradation kinetic triplet parameters were obtained (the activation energy, pre-exponential factor, and function of degree of conversion). The kinetic study was analyzed by means of an integral isoconversional non-isothermal procedure (model free), and the kinetic model was determined by the Coats–Red-fern method and through the compensation effect (IKR). All the systems followed the n = 6 kinetic model. The addition of HAp increases the thermal stability of the systems. The isothermal degradation was simulated from non-isothermal data, and the curing process could be defined to obtain the two types of materials. Temperature under 250 ˚C allows the formation of hybrids networks.

Keywords: Sol gel, HAp, VTES, GPTMS, Kinetics

Introduction

The sol–gel process is a chemical synthesis method initially used for the preparation of inorganic materials such as glasses and ceramics [1]. This process can be described as the creation of an oxide network by progressive condensation reactions of molecular precursors in a liquid medium [2]. Generally, material formation occurs in four stages: (a) hydrolysis, (b) condensation and polymerization of precursors to form chains and particles, (c) growth of the particles, (d) agglomeration of the structures followed by the formation of [3, 4]. Steps b, c, d need to be performed with a thermal treatment that can be named as curing process. Since liquid precursors are used, it is possible to cast coatings in complex shapes and to produce thin films without the need for machining or melting and this method is waste-free and excludes the stage of washing [1–9].

The most widely used metal–organic precursors for the preparation of materials by sol–gel processing are the alkoxysilanes, including tetraoxy silicate (Si $(OR)_4$) and organically modified silicates ($R'n$ $Si(OR)_{4-n}$ or $(RO)_3Si$ $R'Si$ $(OR)_3$, where R is typically an alkyl) [10]. As it is shown in Fig. 1 the sol–gel process of derived silica materials involved the formation of a Si–O–Si network.

Depending on the curing treatment different types of coatings are possible: (a) inorganic (SiO_2) coatings using high temperatures in order to sintherized the film and to degrade the organic compounds and (b) hybrid

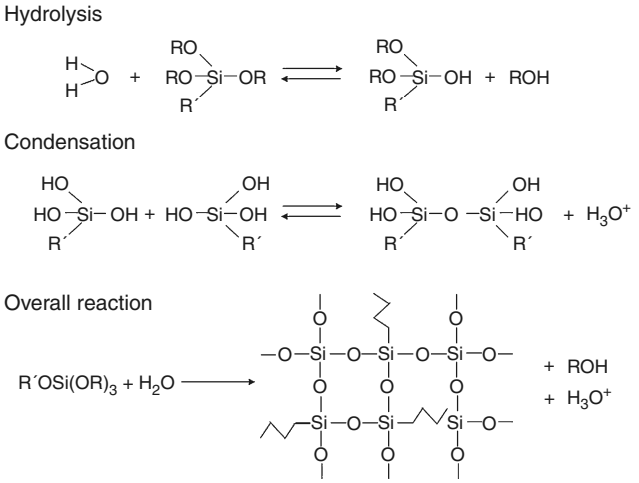

Fig. 1 Hydrolysis and condensation involved in making sol–gel derived silica materials

organic–inorganic sol–gel coatings, in this case we use much lower temperatures.

Inorganic SiO_2 coatings can improve the oxidation and acidic corrosion resistance of metals under different temperatures due to its high heat resistance and chemical resistance [11]. Durán et al. made SiO_2 coating on galvanized steel using tetraethylorthosilicate (TEOS) and methyltriethoxysilane (MTES) precursors to improve the corrosion behaviour of the substrate [6]. Vasconcellos et al. found that the inorganic SiO_2 coating obtained through TEOS was homogeneous, free of cracks and improved the anti-corrosion performance of stainless steel substrate [5]. While inorganic coatings can provide good protection on metal substrates, the drawback of these coatings are brittleness, low thicker and the difficulty to achieve without cracking [1].

To overcome the limitation of pure inorganic sol–gel coatings much works introduce organic chains into the precursors to form the organic–inorganic hybrid coating. Sayilkan et al. developed an organic–inorganic coating on aluminium and iron plates using different alkoxysilanes and they show that in most cases the durability of the coating was satisfactory [7]. Parkhill et al. applied water based epoxide ormosil coatings on aluminium panels using 3-glycidoxypropyl trimethoxysilane (GPTMS) and TEOS as precursors, they characterized film thickness and morphology and evaluated the overall corrosion performance [8]. Chan et al. obtained three kinds of hybrids using TEOS, MTES, vinyltriethoxysilane (VTES) and GPTMS, they demonstrated that the introduction of unhydrolizable organic groups increased the module and the hardness [9]. The group of J.C. Galván have develop hybrid organic–inorganic sol–gel coatings using α-methacryloxypropyltrimethoxysilane (MAP) and tetramethoxysilane (TMOS) loaded with inorganic particles such as titania or cerium that enhance the corrosion properties of sol–gel [12, 13].

On the other hand, one of the most important properties of the silica-based sol–gel system is that they usually have a high content of surface silanol groups, which have been reported to be bone growth inductors because they promote in vitro and in vivo nucleation of apatite. Therefore, they can be used as a coating of orthopaedic metallic implants to overcome the limitations of these materials [10, 11] such as, a limited corrosion resistance in the human body and the lack of bioactivity [14]. The combination of this property with the ability of organic–inorganic systems to embed different bioactive compounds has opened the field of bioactive sol–gel coatings. One way of improving the bioactivity of the sol–gel coatings is adding hydroxyapatite to the sol–gel system (hydroxyapatite particles increase the quality and the bond to the living bone [15]). Most of the works reported around these materials use a high process temperature so the system loses its organic part. Durán et al. have made numerous studies of sol–gel coatings with hydroxyapatite applying sinterization thermal process and they demonstrated the improvement of the corrosion resistance of the substrate and bioactivity [16–18]. Nevertheless, it is possible to use HAp particles in the coating maintaining its organic part, in this case the curing process has to avoid the degradation and of course the sinterization of the film.

In the present study, we report a thermal degradation study of an sol–gel material obtained from glycidyloxypropyltrimethoxysilane (GPTMS) and triethoxyvinylsilane (VTES) with different hydroxyapatite (HAp) particles content. The main objective of this study is to understand thermal degradation kinetics of these materials. Controlling the chemical nature of the initial formulation (precursors and particles), and the curing process we will be able to obtain materials with different organic–inorganic compositions. Moreover, the thermal degradation at high temperatures will be studied and the kinetic model calculated in order to define optimal curing process depending if a hybrid or an inorganic film want to be obtained.

Experimental

Materials

The silica precursors used were glycidyloxypropyltrimethoxysilane (GPTMS) and triethoxyvinylsilane (VTES) from Sigma-Aldrich (used as received). Their chemical structure is shown in Fig. 2.

Isopropanol (Sigma-Aldrich) was used as a co-solvent without further purification.

Fig. 2 Chemical strucuture of glycidyloxypropyltrimethoxysilane (GPTMS) and triethoxyvinylsilane (VTES), respectively

0.1 M nitric acid (HNO_3) was used in order to obtain acidic pH as the catalytic of the hydrolysis and condensation reactions.

The bioactive particles were hydroxyapatite (HAp) particles (>200 nm) from Sigma-Aldrich.

Synthesis of the materials

Synthesis of the inorganic–organic hybrid materials

The GPTMS/VTES sols were prepared by acid catalysis method in one stage. The volume ratio of GPTMS/VTES was 80:20. The precursors were dissolved into isopropanol. The hydrolysis of the alcoxy groups presented in the precursors was carried out by addiction of the stoichiometric quantity of acidified water while stirring at room temperature. The solution were stirred for about 1 h and set for another hour at room temperature before use. The materials were cured at 50 °C for 15 min, 100 °C for 15 min and 140 °C for 90 min (Table 1).

Synthesis of bone grow inductor materials

The bone growth inductors coatings were prepared by the addition of HAp to the organic–inorganic sol–gel coatings. In order to ensure a proper dispersion of the particles in the coating the HAp particles were ultrasonicated Sonoplus HD 3200 in isopropanol before adding to the sol solution. The addition was made after the sol solution was stirring for 1 h and then it was set for another hour at room temperature before use. In this case two materials were prepared 2.5 and 5% HAp wt respect to the precursors. The materials were cured at 50 °C for 15 min, 100 °C for 15 min and 140 °C for 90 min (Table 1).

Characterization and measurements

The Fourier Transform Infrared (FTIR) spectra were recorded with a Thermo Nicolet NEXUS FTIR spectrophotometer in the transmittance mode.

Thermogravimetric analysis (TG) was carried out with Mettler-Toledo TG-50 thermobalance. Cured samples with an approximate mass of 7 mg were degraded between 30 and 700 °C at a heating rate of 10 °C/min in N_2 (100 mL/min) measured under normal conditions. Non-isothermal thermogravimetric tests were carried out at rates of 2, 5, 10 and 20 °C/min to evaluate the kinetic parameters.

The degradation of the materials was performed at the same conditions as TG essays. The residues produced maintaining the materials in different temperatures (240, 450 and 700 °C) were investigated by FTIR spectra in order to follow the degradation of the materials.

Kinetics analysis

Integral non-isothermal kinetic analysis was used to determine the kinetic triplet (A—pre-exponential factor, E—activation energy and $g(\alpha)$—integral function of degree of conversion). The degree of conversion as the mass loss is defined as:

$$\alpha = \frac{m_0 - m}{m_0 - m_\infty} \tag{1}$$

where m is the mass corresponding to temperature T, m_0 is the initial mass and m_∞ is the mass of the substance at the end of the experiment.

If we accept that the dependence of the rate constant on the temperature follows the Arrhenius equation, kinetic analysis may start with the kinetic equation:

$$\frac{\mathrm{d}\alpha}{\mathrm{d}t} = A \exp\left(-\frac{E}{RT}\right) f(\alpha) \tag{2}$$

where $\mathrm{d}\alpha/\mathrm{d}t$ is the rate of conversion, R the universal gas constant, T the temperature and $f(\alpha)$ is the differential conversion function.

Kinetic analysis has generally been performed with an isoconversional method [19]. The basic assumption of such method is that the reaction rate at a constant conversion is solely a function of temperature [20].

Isothermal methods

By integrating the rate equation (Eq. 2) we obtain:

$$\ln t = \ln\left[\frac{g(\alpha)}{A}\right] + \frac{E}{RT} \tag{3}$$

where $g(\alpha)$ is the integral conversion function and is defined as follows:

$$g(\alpha) = \int_0^\alpha \frac{\mathrm{d}\alpha}{f(\alpha)} \tag{4}$$

According to Eq. 3, E and the constant $\ln(g(\alpha)/A)$ can be obtained from the slope and the intercept, respectively, of the linear relationship $\ln t = f(T^{-1})$ for a constant value of α.

Isothermal methods require long times to be performed and give problems with the data acquisition. Firstly, if the degradation is evaluated isothermally at high temperature the reactions take place very fast, the TG equipment was not able to detect the initial mass loss signal because

stabilization time is needed and the initial part of the degradation is lost. Secondly, isothermal experiments at low temperature needs very long time to be performed so, probably non-isothermal data could give more accurate results and easier to obtain than those given by isothermal experiments.

Non-isothermal methods

When non-isothermal methods are applied, the integration of rate equation (Eq. 2) and its reordering gives place to the so-called temperature integral:

$$g(\alpha) = \int_0^{\alpha} \frac{d\alpha}{f(\alpha)} = \frac{A}{\beta} \int_0^{T} e^{-(E/RT)} dT \quad (5)$$

where, β is the heating rate.

By using the Coats–Redfern [21] approximation for the resolution of Eq. 5 and considering $2RT/E \ll 1$, we can rewrite this equation as follows:

$$\ln \frac{g(\alpha)}{T^2} = \ln \left[\frac{AR}{\beta E}\right] - \frac{E}{RT} \quad (6)$$

For a given kinetic model, the linear representation of $\ln[g(\alpha)/T^2]$ versus T^{-1} makes it possible to determine E_{ap} and A from the slope and the ordinate at the origin.

In this study, the kinetic model that had the best linear correlation in the Coats–Redfern equation and that had an E value (E_{ap}) similar to that obtained isoconversionally (considered to be the effective E value, E_{ef}) was selected.

By reordering Eq. 6 the Kissinger–Akahira–Sunose (KAS) equation can be written:

$$\ln \frac{\beta}{T^2} = \ln \left[\frac{AR}{g(\alpha)E}\right] - \frac{E}{RT} \quad (7)$$

The linear representation of $\ln[\beta/T^2]$ versus $1/T$ makes it possible to determine E_{ap} (apparent E value) and the kinetic parameter $\ln[AR/g(\alpha)E]$ for every value of α.

The constant $\ln[AR/g(\alpha)E]$ is directly related by the R/E to the constant $\ln[g(\alpha)/A]$ of the isothermal adjustment. Thus, taking the dynamic data $\ln[AR/g(\alpha)E]$ and E from Eq. 7, we can determine the isothermal parameters of Eq. 3 and simulate isothermal curing without knowing $g(\alpha)$ [22, 23].

Compensation effect and isokinetic relationship (IKR)

Complex processes are characterized by the dependences of E on A and α. This generally reflects the existence of a compensation effect through the following equation:

$$\ln A_\alpha = aE_\alpha + b = \frac{E_\alpha}{RT} + \ln \left[\frac{(d\alpha/dt)_\alpha}{f(\alpha)}\right] \quad (8)$$

where a and b are constants and the subscript α represents the degree of conversion that produces a change in the Arrhenius parameters.

The slope $a = 1/RT_{iso}$ is related to the isokinetic temperature (T_{iso}), and the intercept $b = \ln k_{iso}$ is related to the isokinetic rate constant (k_{iso}). Equation 8 represents an IKR and can be deduced by the reordering of Eq. 2. The appearance of the IKR shows that there is only one model, whereas the existence of parameters that do not meet the IKR (meaning that for a given α the relation between A and E changes) implies that there are several models [24], because $f(\alpha)$ is not constant in all the process.

The kinetic model whose IKR had the best linear correlation between E and A and in which the associated T_{iso} value was near the experimental temperature range was selected [25].

Results and discussion

FTIR analysis

The FTIR analysis provides evidence for the formation of the sol–gel network. Figure 3 shows the FTIR spectra of the GPTMS–VTES hybrid material and Table 2 reports the

Table 1 Materials used in this study their formulation and abbreviation

Material	Formulation	Abbreviation
Inorganic–organic hybrid	GPTMS–VTES	G–V
Bone grow inductor systems	GPTMS–VTES%2.5HAp	G–V2.5HAp
	GPTMS–VTES%5HAp	G–V5HAp

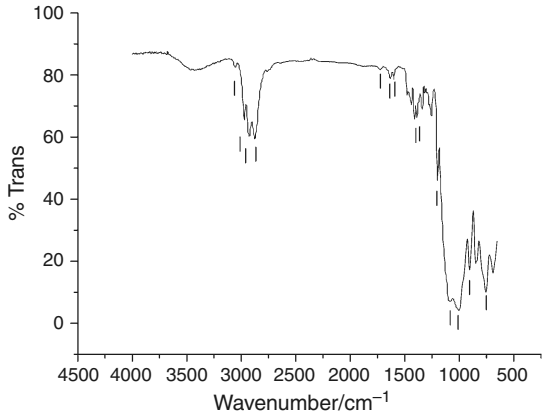

Fig. 3 FTIR spectra of GPTMS–VTES (the wavenumber of marks on the figure are listed in Table 2)

Table 2 Assignment of the FTIR peaks in Fig. 4

Peak position/cm^{-1}	Precursor assignment	Peak assignment
3500	GPTMS and VTES	OH
3061	VTES	CH_2
2989	GPTMS	CH epoxy ring
2939	GPTMS and VTES	Aliphatic
2866	GPTMS	CH_2
1730	GPTMS	C–O epoxy ring
1638	GPTMS	C–C epoxy ring
1594	VTES	Si-Vinyl
1400	VTES	CH2
1384	GPTMS	CH epoxy ring
1205	GPTMS	CH_2–O–CH_2
1070; 1010	GPTMS and VTES	Si–O–Si
912	GPTMS and VTES	Si–OH
763	GPTMS and VTES	Si–O–Si

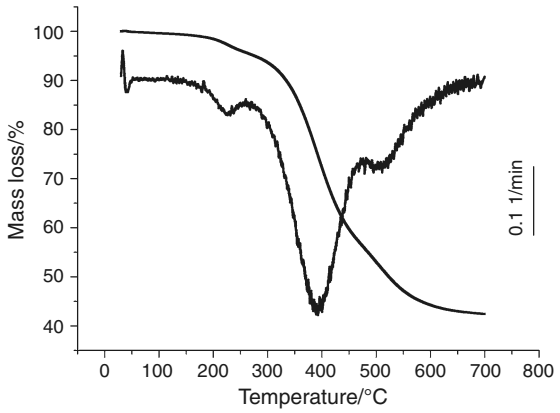

Fig. 4 TG and DTG curves under N_2 atmosphere at 10 °C/min of the G–V material

assignment of the FTIR peaks marked in the spectra with the vibration of the characteristics bonds.

The silica network is characterized by the strong absorptions at 1,070 and 1,010 cm^{-1} corresponding to the Si–O–Si bond. The organic part of the hybrid is characterized by the peaks around 2,500–3,000 cm^{-1}. The epoxy ring reacts partially during the cured process, the main peak 1384 persists but with low intensity. The addition of hydroxiapatite does not change the FTIR spectra, so similar chemical structure it is expected.

Thermal degradation of organic–inorganic hybrid

Figure 4 shows the thermal degradation curve of GPTMS–VTES materials. Three overlapped degradation processes are shown. The first one around 200 °C, the highest mass loss associated with approximately 65% of mass loss is near 400 °C and the last one almost at 550 °C.

In order to understand the degradation process and assign the peaks detected with TG with a specific degradation reaction, a study combining FTIR and TG was carried out. All films were tested in TG at 10 °C/min first until 240 °C (just after first DTG peak), second until 450 °C (after second DTG peak) and third until 700 °C (after third DTG peak). After TG tests the produced residues were investigated by FTIR in order to study the degradation process (Fig. 5).

FTIR analysis of 240 °C sample shows that the intensity of the Si–OH band assign at 912 cm^{-1} compared to FTIR analysis of non-degraded sample has been reduced significatively probably due to the continuation of the condense process and the consequent liberation of the produced alcohols R–OH, so the peaks associated to CH_2 also slightly decrease.

The study of FTIR spectra of 450 °C sample shows that the main loss of mass is due to the degradation of the organic chains of the precursors GPTMS and VTES. All peaks associated to the organic chains (and principally CH_2 and CH) has almost disappeared. Finally FTIR spectra of sample someted to 700 °C shows the decrease of the intensity of the peaks at 1010, 1070 and 763 cm^{-1} that means there has been a degradation of the Si–O–Si network.

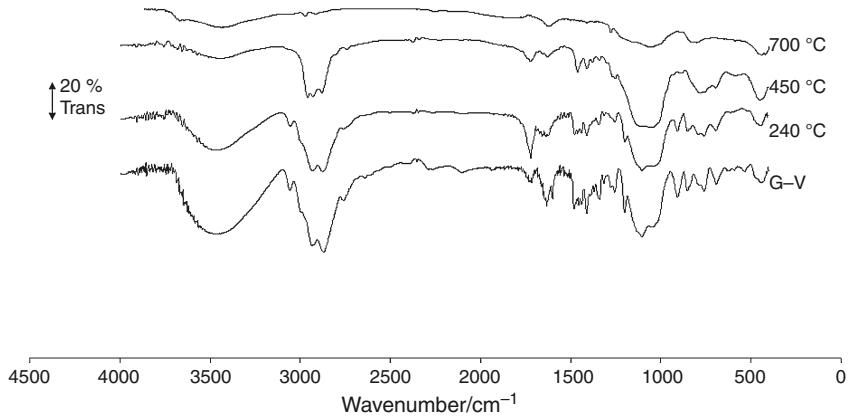

Fig. 5 FTIR spectra of an GPTMS–VTES sample and the residues of same type of sample after TG test at 10 °C/min until the temperatures of 240, 450 and 700 °C

Comparison of the thermal degradation of inorganic–organic hybrid and bone growth inductor systems

Figure 6 shows the TG and DTG curves versus temperature curves of the materials GPTMSVTES and those containing HAp (G–V2.5HAp and G–V5HAp). Table 3 collects some quantitative parameters for these samples obtained directly from the TG raw data.

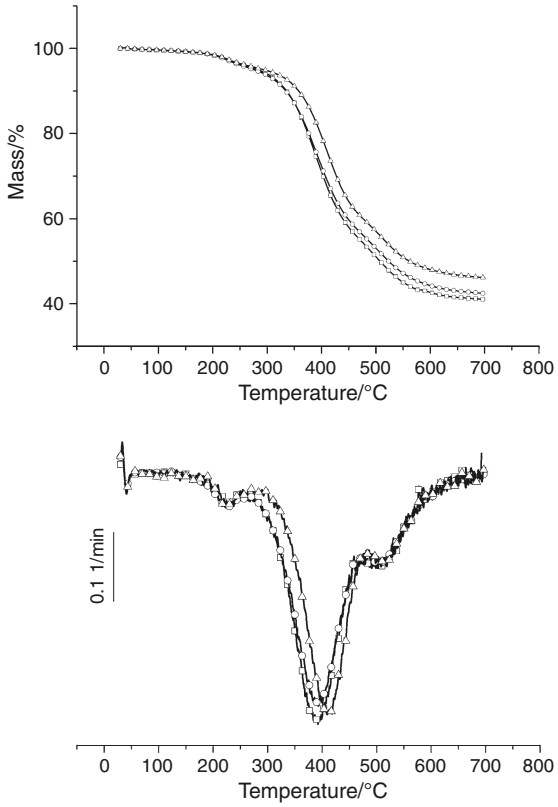

Fig. 6 TG and DTG curves at 10 °C/min in N2 atmosphere of G–V (*filled square*), G–V2.5Hap (*filled circle*) and G–V5Hap (*filled triangle*) samples

Table 3 Thermogravimetric data under N2 atmosphere of G–V, G–V2.5Hap and G–V5Hap

Entry	Formulation	Abbreviation	T_c^a	T_{max}^b	Char yield/%[c]
1	GPTMS:VTES	G–V	373	387	41
2	GPTMS:VTES %2.5 HAp	G–V2.5HAp	378	389	42
3	GPTMS:VTES %5 HAp	G–V5HAp	399	410	46

[a] Temperature of a 20% of weight loss calculated by thermogravimetry

[b] Temperature of the maximum degradation rate calculated by thermogravimetry

[c] Char yield at 700 °C

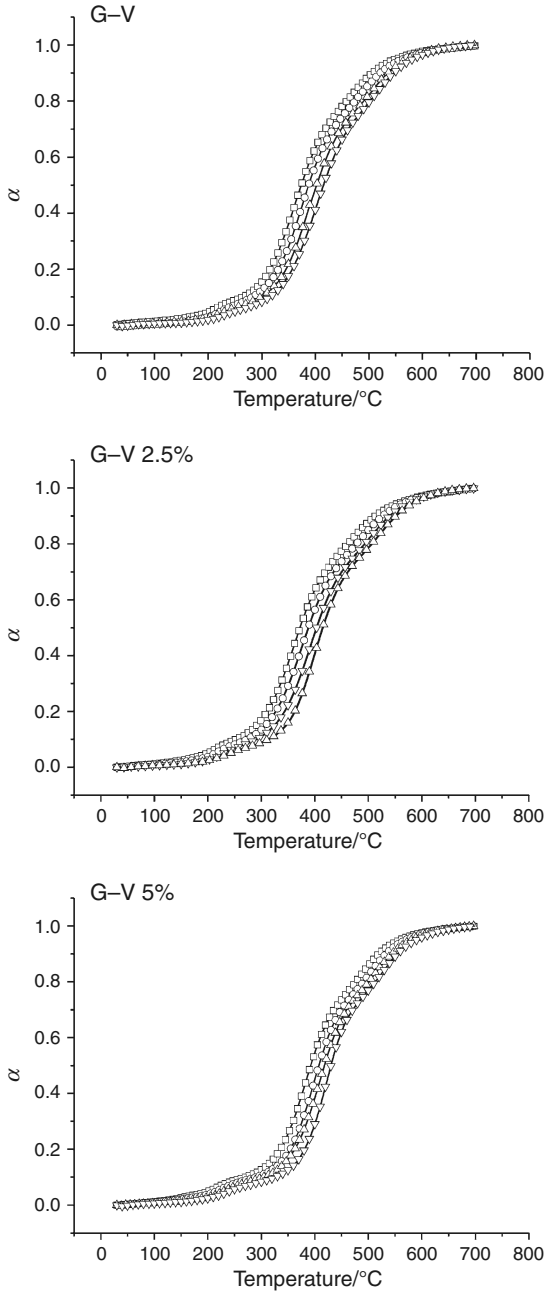

Fig. 7 Thermogravimetric curves at different heating rates (2.5 (*filled square*), 5 (*filled circle*), 10 (*filled triangle*) and 20 (*inverted filled triangle*) °C/min) for each studied material

As it can be seen in Fig. 6, the addition of HAp do not change significantly the degradation process at temperatures lower to 250 °C but modified the thermal degradation process over this temperature. The temperature of maximum degradation rate shifts towards higher temperatures with HAp content, although deeper analysis has to be done to obtain detail analysis.

Data obtained by the thermogravimetric analysis (Fig. 6) was standardized by means of Eq. 1 to find the degree of conversion α versus temperature (Fig. 7) at

different heating rates. The non-isothermal isoconversional kinetic parameters were calculated from α–T curves by the application of the isoconversional KAS equation, Eq. 7, to different conversions, and from these, the isothermal parameter $\ln(g(\alpha)/A)$, with which the studied degradation process would subsequently be simulated. The kinetic analysis was only applied to the main loss peak associate to the degradation of the organic chains of the precursors GPTMS and VTES.

Table 4 shows the kinetic parameters of non-isothermal curing obtained from Eq. 7 for the samples type G–V. The process was repeated with the other two samples containing HAp. Figure 8 shows the experimental relationship between $\ln(\beta/T^2)$ and the inverse of temperature, with the adjustment made with Eq. 7.

In Table 5 it can be seen that activation energy E is modified during the degradation, strongly increasing with the advance of the reaction, probably due to the bigger stability of the bonds as the material degradation proceeds (i.e., Si–O–Si is more stable than Si–C bond). As it can be seen in Table 5 an high increase of HAp content (5% GV) produces an increase of the activation energy E for a given conversion value, whereas a low increase of HAp content (2.5% GV) produces a slightly no regular modification of E. The parameters $\ln(AR/(g(\alpha)E))$ and the associated A value exhibits similar trend.

To establish the kinetic model for system G–V, the isoconversional kinetic parameters (Table 4) and the equation (Eq. 8) were used (the same process was done for the other two formulations with HAp). Different kinetic models were studied: diffusion (D1, D2, D3 and D4), Avrami–Erofeev (A3/2, A2, A3 and A4), power law (P2), phase-boundary-controlled reaction (R2 and R3), reaction-order /n/ (/n/ = 6, 5, 3, 2, 1.5 and 1 denominated F1) and autocatalytic (/n/ + /m/ = 2 with /n/ = 1.5, and /n/ + /m/ = 3 with /n/ = 2.1, 2.3, 2.4, 2.9) [26].

From the parameters $\ln(AR/(g(\alpha)E))$ and E shown in Table 4 and the g(α) functions, A values were calculated for all different kinetics models used. Subsequently, by plotting E versus ln$A$ (Eq. 8), we determined the IKRs for all models used. Table 6 shows the obtained results, as well as the T_{iso} values determined from the slope of the IKRs [27]. The model considered that it is the best one describing the sol–gel material degradation is $n = 6$ because this model shows a good regression and T_{iso} values closer to the experimental procedures. Model $n = 5$ also has a good regression (R^2) and values of T_{iso} close to those found in the isoconversional method, nevertheless, model $n = 6$ correlate better when all the systems are considered globally. In agreement with Vyazovkin and Linert [25], a T_{iso} value close to the range of experimental temperatures indicates that the kinetic model accurately describes the reactive process. The same conclusion was reached for systems with HAp.

To confirm the methodology used with the IKR, we determined E_{ap} and ln$A$ for each tested model with the Coats–Redfern method (Eq. 6) [27, 28]. The results obtained for the sample G–V when Eq. 6 was applied to the conversions related to the high mass loss conversions, are shown in Table 6 (similar results were obtained for the other two samples with HAp and for other heating rates). Some of the models exhibit very good regressions, and so from these data alone, it is not possible to establish the reaction mechanism. To determine the kinetic model, it

Table 4 Kinetic parameters of non-isothermal for GV sample, using the model $n = 6$

α	E/kJ/mol	$\ln[AR/g(\alpha)E]$	$\ln[g(\alpha)/A]$	ln$A$/min^{-1}	R^2
0.2	143.3	17.38	−27.13	26.24	0.9927
0.3	156.5	18.81	−28.66	28.65	0.9943
0.4	166.1	19.72	−29.62	30.48	0.9981
0.5	174.4	20.39	−30.34	32.17	0.9998
0.6	184.3	21.22	−31.22	34.19	0.9996
0.7	197.2	22.13	−32.20	36.61	0.9978
0.8	215.3	23.11	−33.27	39.70	0.9980

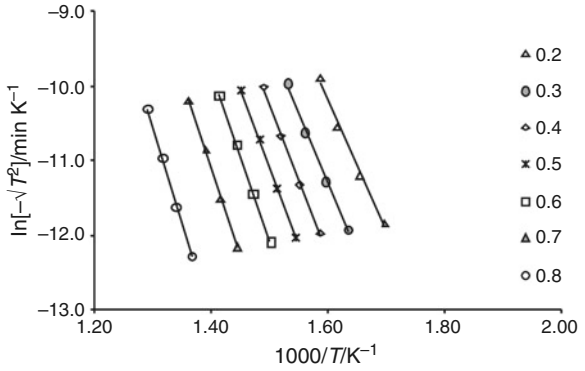

Fig. 8 Parameter $\ln(\beta/T^2)$ versus the inverse of temperature for a sample G–V between 0.2 and 0.8 conversion degree

Table 5 Variation of the activation energy with the conversion of the samples GV and with different (2.5 and 5%) contents of HAp

Conversion	GV	2.5% GV	5% GV
0.2	143.3	114.4	144.4
0.3	156.5	136.6	167.2
0.4	166.1	153.2	185
0.5	174.4	166.4	204.2
0.6	184.3	179	226.3
0.7	197.2	194	251.2
0.8	215.3	205.5	270.8

Table 6 Arrhenius parameters determined by the Coats–Redfern method and isokinetic parameters for a G–V sample at a heating rate of 10 °C/min

Models	Coats–Redfern			IKR			
	E	$\ln A/\text{min}^{-1}$	R^2	a	b	T_{iso}/°C	R^2
A3/2	24.6	1.33	0.9476	0.103	11.772	889.0	0.9828
A2	15.6	−0.65	0.9259	0.099	12.664	943.5	0.9833
A3	6.6	−3.04	0.8241	0.094	13.555	1003.4	0.9838
A4	2.1	−4.95	0.4393	0.092	14.000	1035.6	0.9840
R2	33.4	2.17	0.9312	0.110	9.322	824.1	0.9801
R3	36.3	2.43	0.9429	0.108	9.924	838.9	0.9793
D1	62.6	7.73	0.9213	0.124	6.934	700.2	0.9711
D2	83.5	13.08	0.9562	0.128	5.612	663.9	0.9734
D3	84.0	10.09	0.9582	0.134	3.307	622.5	0.9767
D4	76.1	8.42	0.9471	0.130	3.844	649.8	0.9746
F1	42.6	4.93	0.9616	0.113	9.990	793.4	0.9819
Power	7.1	−3.12	0.6851	0.095	13.236	998.3	0.9809
$n = 1.5$	53.2	7.24	0.9800	0.118	9.250	745.1	0.9848
$n = 2$	65.3	9.80	0.9904	0.124	8.402	695.4	0.9878
$n = 3$	93.1	15.56	0.9979	0.138	6.417	597.3	0.9931
$n = 5$	159.3	28.93	0.9964	0.171	1.673	428.6	0.9985
$n = 6$	195.4	36.14	0.9947	0.189	−0.913	361.6	0.9992
$n = 2.1$, $m = 0.9$	4.1	−1.40	0.9516	0.093	16.355	1021.8	0.9891
$n = 2.3$, $m = 0.7$	28.2	3.86	0.9968	0.105	13.236	870.6	0.9917
$n = 2.4$, $m = 0.6$	38.7	5.78	0.9979	0.110	12.063	815.7	0.9922
$n = 2.9$, $m = 0.1$	84.5	14.04	0.9980	0.134	7.274	625.6	0.9931

was also used the average value of E obtained isoconversionally shown in Table 5. This value of E is considered the effective value because it was obtained without the necessity of determining the model. In addition to the good regression, the correct kinetic model must also possess a value of E similar to the effective value. According to these criteria model $n = 6$, with good regression and E value closer to the E_{ef} in the three samples, is considered the correct one for samples with and without HAp. Other similar models such $n = 5$ can also describe the curing.

All the samples investigated showed that the two methodologies (IKR and Coats–Redfern) lead to the same result, and in both cases, it is necessary to know the effective E (isoconversional) value to determine the complete kinetic triplet (E, A and $f(\alpha)$) [23].

If we compare the activation energies (Table 5), a simple analysis would conclude that the fastest system considering degradation is that with the minor E, but this is not always true because a compensation effect between E and ln$A$ exists [29]. Then, to know which is the most efficient system it should be compared the rate constant, k (because samples fit the same kinetic model $g(\alpha)$). Eq. 9 shows the Arrhenius relation between k (rate constant), A and E.

$$k = A \cdot \exp\left(-\frac{E}{RT}\right) \rightarrow \ln k = \ln A - \frac{E}{RT} \tag{9}$$

Introducing in Eq. 9 values of E, A and α with the chosen kinetic model $n = 6$ and for a given conversion degree ($\alpha = 0.5$) we can obtain a graphic like Fig. 9 ($\ln k = f(1/T)$).

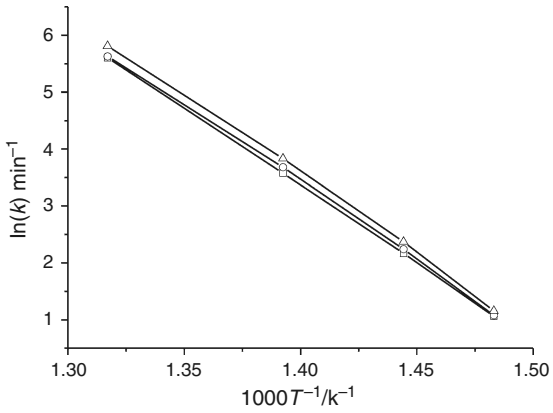

Fig. 9 Rate constant, ln k, versus the inverse of temperature (1000/T) for G–V (*filled square*), G–V2.5HAp (*filled circle*) and G–V5HAp (*filled triangle*) samples

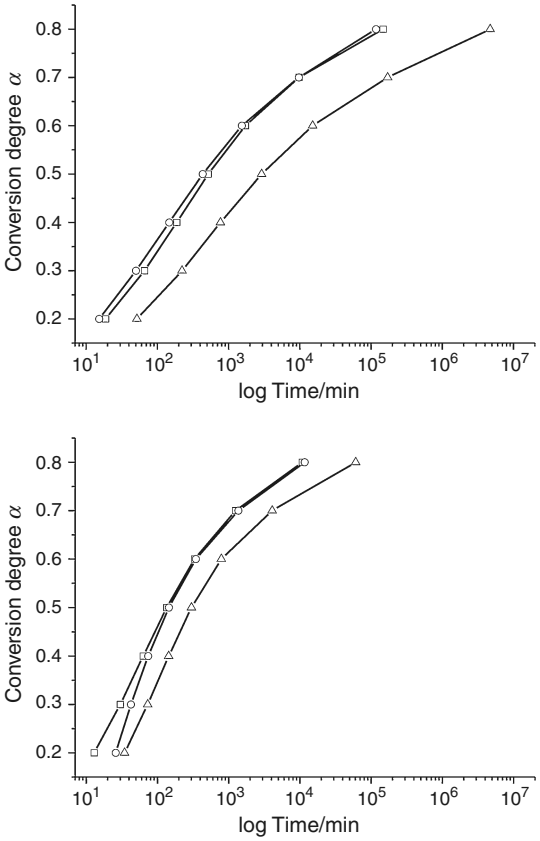

Fig. 10 Predicted evolution of weight loss against time at 300 and 400 °C of inorganic–organic hybrid system with and without Hap G–V (*filled square*), G–V2.5Hap (*filled circle*) and G–V5Hap (*filled triangle*) samples

In this figure, it can be observed that the addition of HAp decrease the rate constant which means that these systems are more stable with a reduction of the degradation rate with temperature. These results corroborate that in order to know which system could be more stable at determined temperature it is appropriate to consider not only E but also the parameter ln$A$ if they fit the same kinetic model [27, 28].

Finally, by applying the isoconversional procedure, Eq. 3, we can predict the time necessary to reach a determined degree of mass loss at a selected temperature. Figure 9 shows the plot of mass loss against time at 300 and 400 °C for the different formulations. We have found that the simulated time are similar to those obtained isothermally. These results suggest that the methodology used in this study is correct and could be used to simulate isothermal degradation at other temperatures (Fig. 10).

As it can be seen in Fig. 10, the more thermal stable systems are those with higher HAp content (at a specific temperature the mass losses at a time is less as hydroxyapatite increase). The reason for this procedure can be that the addition of HAp stabilizes the network formed by sol–gel process specially when its content is 5% wt.

Conclusions

In order to optimize the curing procedure for hybrid systems to obtain Si networks with or without organic chains, a thermal degradation TG test has been developed. Different types of samples were prepared by sol–gel process with the alkoxysilanes GPTMS and VTES, with different amount of HAp (0, 2.5 and 5% w/w).

Combining FTIR and TG tests it was possible to obtain better description of the degradation mechanism. Degradation process starts with the loss of low molecular mass polymer chains as CH2 around 200 °C, continuing after 250 °C with the main degradation process with total loss of the organic chains and finally after 450 °C the degradation of the Si–O–Si network.

Two methods (Coats–Redfern and IKR) that allows the determination of the complete kinetic triplet (E, A, $g(\alpha)$) have been applied. The effective E value has to be known, which can be determined with an isoconversional procedure (model-free).

All systems showed that the reaction mechanism followed an $n = 6$ model, showing no dependence of the HAp quantity. Degradation rates for all the systems were obtained and the results showed that adding HAp, systems are more thermal stable.

After the numerical modelization of the degradation process, with the knowing of the kinetic triplet, it is possible to optimize de curing treatment. It is possible to determine the temperature and time conditions to obtain total inorganic material or hybrids ones. For example, curing temperatures under 200 °C will lead to an hybrids network. In order to obtain an inorganic network, it will be necessary to calculate isothermal degradation curves as those showed in Fig. 10. If we apply curing temperatures around 300 °C, the time needed to obtain the inorganic network will be 10^5 min for samples without HAp or 2.5% HAp, and more than 10^6 for samples with 5% HAp.

References

1. Wen JY, Wilkes GL. Organic/inorganic hybrid network materials by the sol–gel approach. Chem Mater. 1996;8:1667–81.
2. Brinker CJ, Scherer GW. Sol–gel science: the physics and chemistry of sol–gel processing. London: Academic Press; 1990.
3. Guglielmi M. Sol–gel coatings on metals. J Sol–Gel Sci Technol. 1997;8:443–9.
4. Wright JD, Sommerdijk N. Sol–gel materials chemistry and applications. London: CRC Press; 2001.

5. Vasconcelos DCL, Carvalho JAN, Mantel M, Vasconcelos WL. Corrosion resistance of stainless steel coated with sol–gel silica. J Non-Cryst Solids. 2000;273:135–9.
6. Conde A, De Damborenea J, Duran A, Menning M. Protective properties of a sol–gel coating on zinc coated steel. J Sol–Gel Sci Technol. 2006;37:79–85.
7. Sayilkan H, Sener S, Sener E, Sulu M. The sol–gel synthesis and application of some anticorrosive coating materials. Mater Sci. 2003;39:733–9.
8. Parkhill RL, Knobbe ET, Donley MS. Application and evaluation of environmentally compliant spray-coated ormosil films as corrosion resistant treatments for aluminum 2024-T3. Prog Org Coat. 2001;41:261–5.
9. Chan Z, Ai'mei L, Xiao Z, Miao F, Juan H, Hongbing Z. Microstructures and properties of ORMOSIL comprising methyl, vinyl, and [gamma]-glycidoxypropyl-substitued silica. Opt Mater. 2007;29:1543–7.
10. Li PJ, Ohtsuki C, Kokubo T, Nakanishi K, Soga N, Nakamura T, Yamamuro T. Apatite formation induced by silica-gel in a simulated body-fluid. J Am Ceram Soc. 1992;75:2094–7.
11. Kawashita M, Nakao M, Minoda M, Kim HM, Beppu T, Miyamoto T, Kokubo T, Nakamura T. Apatite-forming ability of carboxyl group-containing polymer gels in a simulated body fluid. Biomaterials. 2003;24:2477–84.
12. Chico B, Galván JC, de la Fuente D, Morcillo M. Electrochemical impedance spectroscopy study of the effect of curing time on the early barrier properties of silane systems applied on steel substrates. Prog Org Coat. 2007;60:45–53.
13. Garcia-Heras M, Jimenez-Morales A, Casal B, Galvan JC, Radzki S, Villegas MA. Preparation and electrochemical study of cerium-silica sol–gel thin films. J Alloys Compd. 2004;380: 219–24.
14. Galliano P, De Damborenea JJ, Pascual MJ, Duran A. Sol–gel coatings on 316L steel for clinical applications. J Sol–Gel Sci Technol. 1998;13:723–7.
15. Ohtsuki C, Miyazaki T, Tanihara M. Development of bioactive organic–inorganic hybrid for bone substitutes. Mater Sci Eng C. 2002;22:27–34.
16. García C, Ceré S, Durán A. Bioactive coatings prepared by sol–gel on stainless steel 316L. J Non-Cryst Solids. 2004;348:218–24.
17. García C, Ceré S, Durán A. Bioactive coatings deposited on titanium alloys. J Non-Cryst Solids. 2006;352:3488–95.
18. Ballarre J, Lopez DA, Rosero NC, Duran A, Aparicio M, Cere SM. Electrochemical evaluation of multilayer silica-metacrylate hybrid sol–gel coatings containing bioactive particles on surgical grade stainless steel. Surf Coat Technol. 2008;203:80–6.
19. Salla JM, Cadenato A, Ramis X, Morancho JM. Thermoset cure kinetics by isoconversional methods. J Therm Anal Calorim. 1999;56:771–81.
20. Vyazovkin S, Wight CA. Kinetics in solids. Annu Rev Phys Chem. 1997;48:125–49.
21. Coats AW, Redfern JP. Kinetic parameters from thermogravimetric data. Nature. 1964;201:68.
22. Ramis X, Salla JM, Cadenato A, Morancho JM. Simulation of isothermal cure of a powder coating—non-isothermal DSC experiments. J Therm Anal Calorim. 2003;72:707–18.
23. Ramis X, Cadenato A, Salla JM, Morancho JM, Valles A, Contat L, Ribes A. Thermal degradation of polypropylene/starch-based materials with enhanced biodegradability. Polym Degrad Stab. 2004;86:483–91.
24. Vyazovkin S, Linert W. The application of isoconversional methods for analyzing isokinetic relationships occurring at thermal-decomposition of solids. J Solid State Chem. 1995;114: 392–8.
25. Vyazovkin S, Linert W. False isokinetic relationships found in the nonisothermal decomposition of solids. Chem Phys. 1995; 193:109–18.
26. Chrissafis K. Kinetics of thermal degradation of polymers. J Therm Anal Calorim. 2009;95:273–83.
27. Garcia SJ, Serra A, Ramis X, Suay J. Influence of the addition of erbium and ytterbium triflates in the curing kinetics of a DGEBA/*o*-tolybiguanide powder mixture. J Therm Anal Calorim. 2007;89:223–31.
28. Garcia SJ, Ramis X, Serra A, Suay J. Cationic crosslinking of solid DGEBA resins with ytterbium(III) trifluoromethanesulfonate as initiator. J Therm Anal Calorim. 2006;83:429–38.
29. Salla JM, Morancho JM, Cadenato A, Ramis X. Non-isothermal degradation of a thermoset powder coating in inert and oxidant atmospheres. J Therm Anal Calorim. 2003;72:719–28.